NTIA Report 02-391

Analysis of the RF Threat to Telecommunications Switching Stations and Cellular Base Stations

John J. Lemmon
Roger A. Dalke

U.S. DEPARTMENT OF COMMERCE
Donald L. Evans, Secretary

Nancy J. Victory, Assistant Secretary
for Communications and Information

February 2002

CONTENTS

ANALYSIS OF THE RF THREAT TO TELECOMMUNICATIONS SWITCHING STATIONS AND CELLULAR BASE STATIONS

John J. Lemmon and Roger A. Dalke[1]

The objective of this report is to assess the vulnerability of telecommunications switching stations and cellular base stations to high power electromagnetic radiation generated by an RF device. Analyses, measurements, and simulations of indoor propagation and the penetration of electromagnetic fields into structures indicate that typical buildings provide little, if any, protection for telecommunications switching stations from high power electromagnetic fields. The front end electronics of cellular base stations are also vulnerable to damage from high intensity RF fields via front door coupling through the receive antennas. Tools to provide estimates of power densities inside of structures and the received power levels in cellular base stations are developed in this report. More quantitative predictions of field strengths inside structures require detailed analyses on a case-by-case basis. The techniques to carry out such analyses are currently available and are briefly discussed.

Key words: critical infrastructure protection, high power RF fields, telecommunications switching stations, cellular base stations, shielding, vulnerability

1. INTRODUCTION AND BACKGROUND

In a previous report [1] it was pointed out that high level electromagnetic fields can upset and damage electronics, as well as disrupt or disable computer software (see also [2]). High power radio frequency (RF) fields could therefore pose a threat to critical infrastructures that depend on electronic equipment, such as public and private telecommunications networks. Moreover, RF devices that are designed to disrupt electronic equipment have been developed and represent an emerging threat to the telecommunications infrastructure [3,4]. The objective of [1] was to perform a brief assessment of the vulnerability of public and emergency telecommunications systems to high intensity RF fields. In particular, the following questions were addressed:

> Can the loss of a node (or nodes) cascade through the telecommunications network causing a large-scale system blackout or crash?

[1] The authors are with the Institute for Telecommunication Sciences, National Telecommunications and Information Administration, U.S. Department of Commerce, Boulder, CO 80305.

Can high intensity RF fields disrupt or disable a node (such as a switching station or a wireless base station)?

The basic conclusions that were reached are:

The overall public telecommunications network has sufficient redundancy and capacity to withstand the loss of even multiple nodes. A full nationwide system collapse is not envisioned as a possible scenario. Loss of equipment or failure of software at a telecommunications switching station or a wireless base station could lead to a large local blackout, but is not likely to cascade further within the system.

Neither public network switching stations nor cellular base stations are intentionally hardened against high intensity RF fields, and the shielding provided by concrete and re-bar construction is negligible for wavelengths on the order of, or smaller than, the re-bar spacing. A switching station could therefore be disrupted, although the probability of disruption is difficult to assess due to the variety and complexity of building layouts. Wireless base stations are highly vulnerable to high power devices operating within the base station pass band due to front door antenna coupling.

These conclusions were based on a review of telecommunications networks, discussions with providers, and basic estimates of the coupling of RF energy into telecommunications systems. However, to more accurately assess the vulnerability of these systems to high intensity RF fields, more detailed modeling and measurements are needed. In particular, a model of the transfer function relating a source external to a building and equipment internal to a building needs to be developed. This would more accurately define the threat to equipment located within buildings.

In this report, tools that can be used to estimate the threat to telecommunications equipment are presented. The report is organized as follows. In Section 2 electromagnetic models of the penetration of RF energy into structures are discussed. The most basic penetration models, infinite slab models, are introduced first, and the loss of RF energy as a function of frequency, slab thickness, and electrical conductivity is discussed for both homogeneous and heterogeneous slab materials. Next, penetration via apertures in infinite slabs is discussed, with attention given to the different analytical approximations that are appropriate for the different regimes of aperture dimension relative to a wavelength. Finally, the propagation of RF energy in the interior of a structure is considered, and a model of indoor propagation is developed. It is pointed out that the model predictions are consistent with measurements and simulations of indoor propagation.

Having discussed the penetration of RF energy into structures not intended to collect electromagnetic energy in Section 2, the coupling of energy into cellular base stations via the base station receive antennas is discussed in Section 3.

In Section 4 the results of Sections 2 and 3 are condensed into analysis tools that can be used to predict received power levels inside structures that house telecommunications equipment and in cellular base stations.

Section 5 summarizes the results.

2. METHODS FOR ESTIMATING WORST CASE ELECTROMAGNETIC THREAT LEVELS INSIDE OF BUILDINGS OR OTHER ENCLOSURES

Often, telecommunications equipment that may be subjected to damage from high intensity RF fields will be inside some type of building or enclosure. Hence, it is important to understand the level of RF shielding thus provided and the effects of propagation in complicated indoor environments. Due to the wide variety of building practices and materials and the complicated nature of electromagnetic wave interactions, simplified models are needed to estimate inherent shielding due to structures housing telecommunications equipment. In this section we describe electromagnetic coupling and propagation models and their utility in estimating the potential RF threat to telecommunications equipment.

2.1 Infinite Slab Model

Perhaps the simplest model that can be used to estimate the electromagnetic shielding provided by a building wall is the infinite slab model. With this model, the worst case interior electromagnetic fields due to a source exterior to a building or structure are estimated by using the transfer function for a plane wave impinging on an infinite slab of finite conductivity. The slab can be homogeneous with respect to the wavelengths of interest (e.g., concrete) in which case analytic solutions are available, or inhomogeneous (e.g., reinforced concrete) in which case numerical or other approximate techniques are required.

The transfer function for a plane wave normally incident on an infinite homogenous slab of thickness d in free space is [1]

$$\frac{E_{trans}}{E_{inc}} = \frac{4e^{-ikd}}{(1-k_s/k)(1-k/k_s)e^{ik_sd} + (1+k_s/k)(1+k/k_s)e^{-ik_sd}}$$

where $k = \omega\sqrt{\varepsilon_0\mu_0}$ is the free space propagation constant, $k_s = \sqrt{\omega^2\varepsilon\mu + i\sigma\omega\mu}$ is the propagation constant for the slab, $\omega = 2\pi f$ is the circular frequency, and the parameters ε, μ, and σ are the electromagnetic permittivity, permeability, and conductivity of the slab. The transmission coefficient is obtained by squaring the absolute value of the above expression. The salient features of this expression can best be described by an example calculation as shown in Figures 1 and 2. In Figure 1, the transmission coefficient as a function of frequency is given for conductivities of 0, 1, and 10 mS/m, a relative permittivity of 6, and $d = .2032$ m. In Figure 2, the transmission coefficient is given as a function of thickness at a frequency of 1 GHz.

Figure 1 shows that when the conductivity is 1 mS/m or less, at best there is only moderate attenuation and at worst (when the thickness is an integer number of half wavelengths) there is essentially no attenuation. It is expected that many common building materials such as concrete, brick, wood, gypsum, glass, marble, etc., are poor conductors with microwave conductivities of a few mS/m or less, and hence the shielding over a broad range of frequencies can be considered to

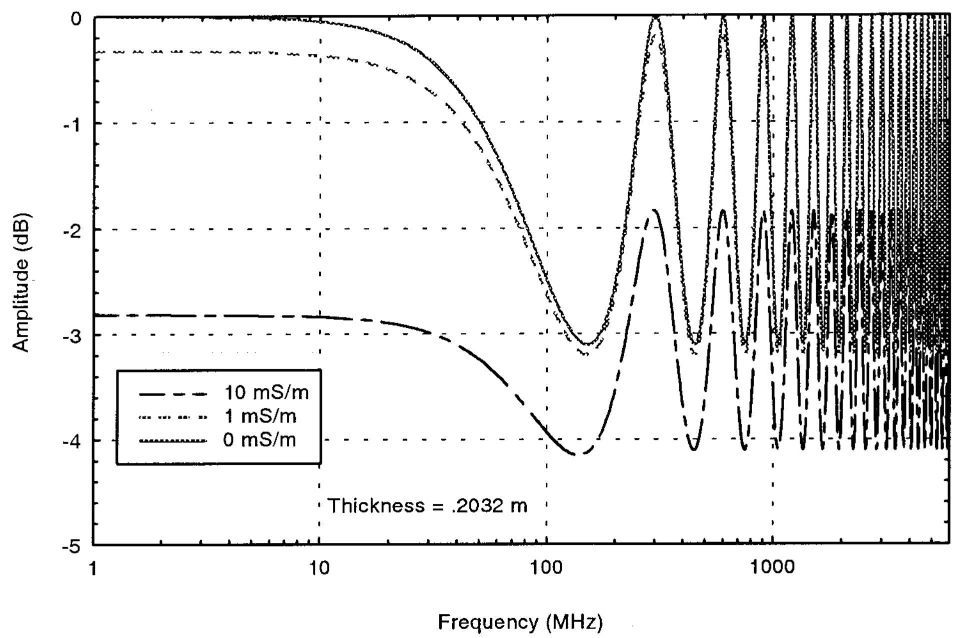

Figure 1. Transmission coefficient as a function of frequency for a slab 20.32 cm thick and 0, 1, and 10 mS/m.

be negligible. Figure 2 shows the same results for a single frequency (1 GHz) as a function of wall thickness. As before, when the thickness is an integer number of half wavelengths the attenuation is small and even in the best of circumstances, the wall only provides minimal shielding.

Steel reinforcing is often used to augment the strength of building walls. The presence of highly conducting materials in otherwise poor conductors, such as reinforced concrete, can provide a degree of shielding at various frequencies depending on the structural geometry. In some cases, an infinite slab model can be used to obtain an estimate of the electromagnetic shielding provided by such structures. For example, electromagnetic penetration of reinforced concrete walls can be estimated by utilizing an infinite slab model containing a periodic screen or lattice of perfect conductors representing the reinforcing structure. Tractable closed form solutions for such models are difficult to obtain and numerical methods are often required to calculate electromagnetic wave interactions.

Numerical methods have been used to analyze the reflection and transmission coefficient for a plane wave normally incident on a 2-dimensional periodic rebar lattice embedded in a concrete wall (see Figure 3) [2]. These results provide a general illustration of the electromagnetic field behavior in the presence of an infinite slab of reinforced concrete. Figure 4 shows the transmission coefficient for a periodic rebar lattice in free space. The lattice has a period (2-dimensional) of 7.62 cm. At low frequencies, the lattice acts inductively and the transmitted field strength increases with frequency to a maximum at the first resonance where the wavelength is approximately equal to the lattice period. It should be noted that the shape of the curves as well as the wavelength of the first resonance are in general a function of the rebar diameter as well as the lattice dimensions.

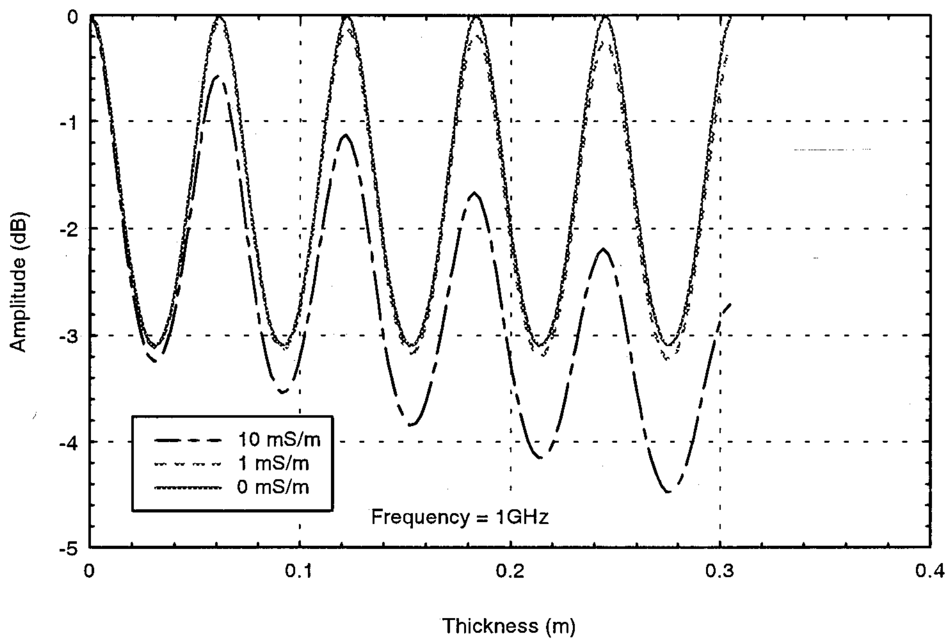

Figure 2. Transmission coefficient as a function of slab thickness at 1 GHz and 0, 1, and 10 mS/m.

The transmission coefficients for reinforced concrete walls of various thickness are given in Figures 5-7. In these examples, the concrete has a conductivity of 1.95 mS/m and a relative permittivity of 6 (typical for concrete at approximately 1 GHz [3]). The rebar lattice attenuates the low frequencies as with the free space model. The first peak in the transmission coefficient roughly corresponds to the frequency of the first resonance of a slab without a reinforcing structure (i.e., the wavelength of the first resonance is about twice the wall thickness). The following peaks are not at even integer multiples of the first resonance (as would be the case in the absence of a reinforcing structure) and are due to the interaction between the wall and the reinforcing structure. It should be noted that after the first peak, the reinforced concrete wall has generally larger transmission coefficients than the rebar lattice alone. Also, the frequency dependence is much more complicated than that of a lattice in free space.

While actual building practices may utilize reinforcing lattice structures having geometries that are different from the previous examples, it is expected that the behavior over a broad range of frequencies will be similar. That is, frequencies with wavelengths that are greater than the characteristic dimensions of the lattice will be attenuated. At higher frequencies, the attenuation will be a complicated function of frequency ranging from tens of dB to nearly 0 dB for resonant frequencies. Hence, it is expected that such structures will not provide significant protection for many frequencies with wavelengths that are on the order of or smaller than the characteristic dimensions of the reinforcing structure.

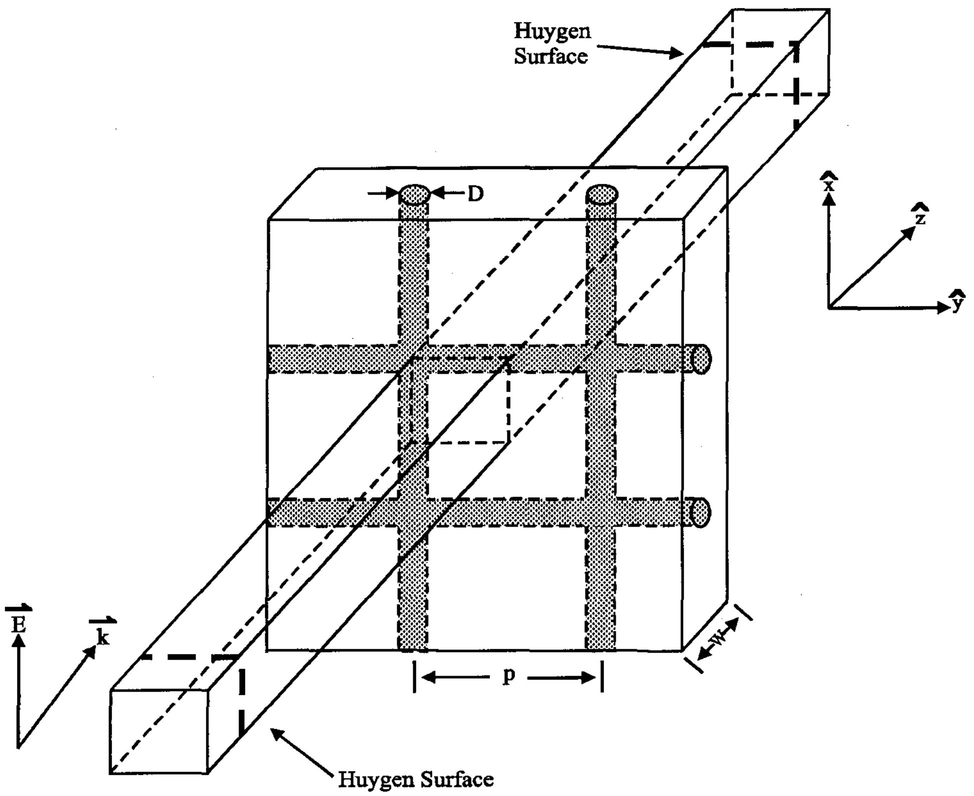

Figure 3. Reinforced concrete wall structure used to calculate transmission coefficients shown in Figures 4-7.

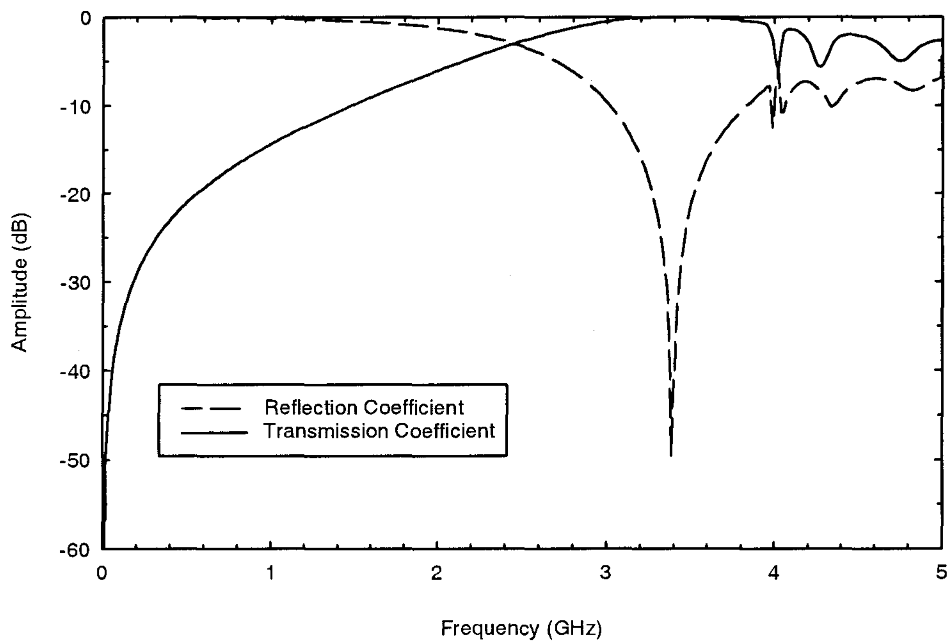

Figure 4. Transmission coefficient for a 2-dimensional lattice in free space (P=7.62 cm and D=1.91 cm).

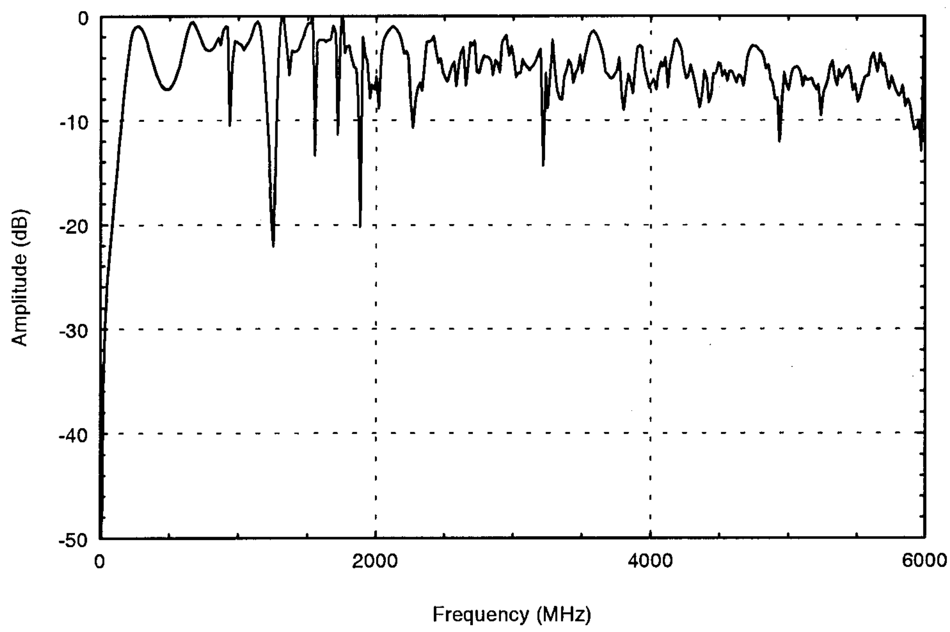

Figure 5. Transmission coefficient for a reinforced concrete wall (P=15.24 cm, D=1.91 cm, and W=20.32 cm).

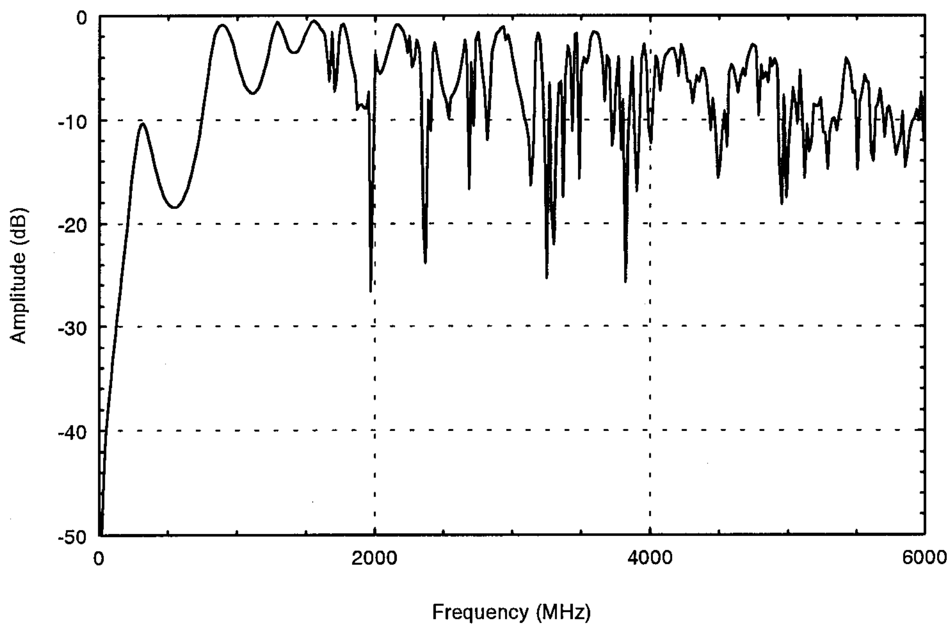

Figure 6. Transmission coefficient for a reinforced concrete wall (P=7.62 cm, D=1.91 cm, and W=20.32 cm).

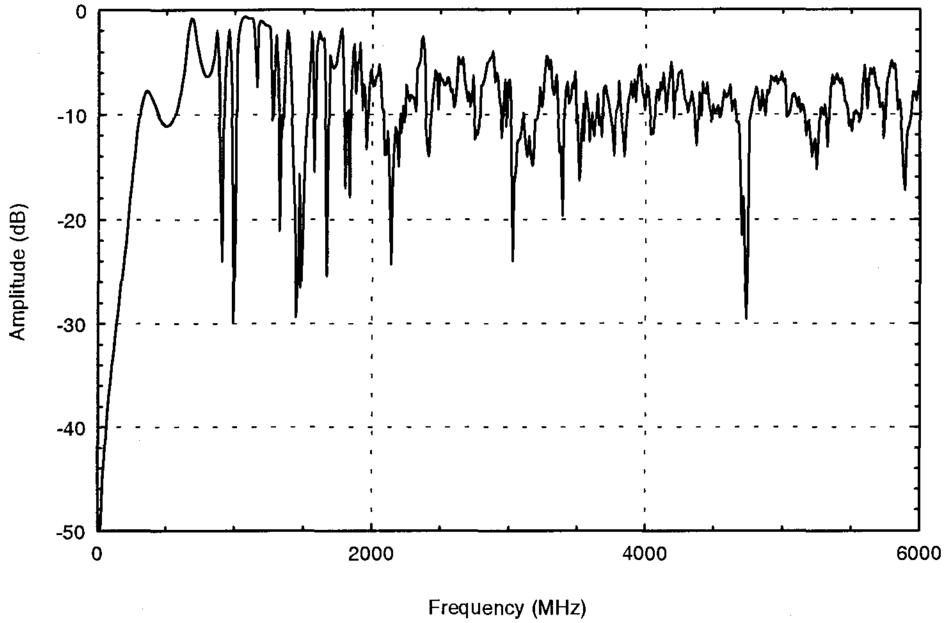

Figure 7. Transmission coefficient for a reinforced concrete wall (P=15.24 cm, D=5.08 cm, and W=20.32 cm).

Various wall attenuation measurements have been reported in the literature; however, each particular measurement only applies to the specific frequency, construction materials, and geometry used in the experiment. As noted in [4], exact models for penetration are difficult to determine, as only a limited number of experiments have been published. For the worst case scenario, the models presented above suffice to show that in general, it should be assumed that very little protection is afforded when the building materials are comprised primarily of poorly conducting materials and the RF threat covers a broad range of frequencies.

2.2 Coupling via Apertures

The results presented above show that walls constructed of materials with poor conductivities (a few mS/m or less) may allow considerable electromagnetic wave penetration at various microwave frequencies. Since buildings constructed of such materials do not provide much shielding, the presence of windows, doors, open access holes, cracks, seams, etc., is not a significant issue. Such wall penetrations become important, however, when the building construction includes intentional shielding, in which case a significant contribution to the interior electromagnetic field levels can be due to aperture penetration. The following discussion is intended to provide an overview of methods that can be used to estimate the transmission of electromagnetic radiation via apertures. As before, the shielding properties of walls with apertures may be estimated by examining the more tractable problem of an electromagnetic wave impinging on an infinite perfectly conducting sheet containing an aperture.

The aperture diffraction problem is divided into two regimes depending on the distances from the source and observation points to the aperture. When the source and observation points are at distances that are much greater than the ratio of the square of the largest aperture dimension to the wavelength of the incident field, the Fresnel-Kirchoff diffraction integral is greatly simplified. This regime is known as Fraunhoffer diffraction [9]. The converse case is known as Fresnel diffraction. The Fresnel diffraction problem is much more difficult with few analytic solutions. Various algorithms have recently been developed for solving the Fresnel diffraction problem [10] including a formulation using Feynman path integrals [11].

When the aperture opening is large compared to a wavelength (i.e., electrically large), the main part of the wave passes through the opening in the manner of geometrical optics and only slight diffraction effects occur. If the aperture is on the order of a wavelength, numerical methods will most likely be required to obtain an accurate estimate of the field intensity for the case of Fresnel diffraction. It is expected that in most cases where buildings or other structures are designed with intentional shielding, aperture sizes will likely be much smaller than the shortest wavelength for which the shielding was designed. In any event, a reasonable worst case estimate for aperture dimensions on the order of or greater than a wavelength can be made by assuming that the electromagnetic waves pass through the aperture unperturbed.

When the dimensions of the aperture are much less than the smallest RF threat wavelength (i.e., electrically small), the radiated fields that penetrate the aperture can be approximated as those due to equivalent electric $\vec{p}$ and magnetic $\vec{m}$ dipoles [12, 13]. The equivalent dipoles are calculated using *short circuit* electric $\vec{E}^{(sc)}$ and magnetic $\vec{H}^{(sc)}$ fields (i.e., fields at the surface of an infinite perfectly conducting plane without an aperture) and geometrical factors known as *polarizabilities.*

The electric dipole moment is normal to the aperture, and hence the electric polarizability, γ^E, is a scalar quantity. The magnetic dipole is in the plane of the aperture and in general, the magnetic polarizability, γ^M, is a 2×2 tensor. The magnetic tensor can be diagonalized by choosing the appropriate principal axes for the aperture geometry. There are thus three polarizabilities (one electric and two magnetic). The equivalent dipole sources can be written

$$\vec{p} = \varepsilon \gamma^E \vec{E}^{(sc)}$$

$$m_\alpha = \sum_\beta \gamma^M_{\alpha\beta} H^{(sc)}_\beta .$$

Polarizabilities for a wide variety of shapes are given in [13]. For a circular aperture, the polarizabilities are

$$\gamma^{E} = \frac{-d^3}{6}$$

$$\gamma^{M}_{\alpha\beta} = \frac{d^3}{3}\delta_{\alpha\beta}$$

where d is the diameter of the aperture. The radiated fields due to the electric dipole are

$$\vec{H} = \frac{\omega^2}{4\pi c}\psi\, \hat{n}\times\vec{p}$$

$$\vec{E} = \eta_0 \vec{H}\times\hat{n}$$

and the fields due to the magnetic dipole are

$$\vec{E} = \frac{\eta_0 k^2}{4\pi}\psi\, \vec{m}\times\hat{n}$$

$$\vec{H} = \frac{1}{\eta_0}\hat{n}\times\vec{E}$$

where c is the speed of light in a vacuum, η_0 is the free space impedance, $\psi = e^{ikX}/X$, $\hat{n} = \vec{X}/X$, $X = |\vec{X}|$, and $\vec{X}$ is the vector from the source to the observation point.

As an example, consider a linearly polarized plane wave normally incident on a conducting sheet with an electrically small circular hole. The magnitudes of the equivalent dipoles are $|\vec{p}| = 0$, $|\vec{m}| = 2|\vec{H}_{inc}|d^3/3$ where d is the diameter of the aperture and $\vec{H}_{inc}$ is the incident magnetic field. The interior fields are equivalent to the fields radiated from a magnetic dipole located at the aperture with the magnetic dipole moment vector in the plane of the conducting sheet. At distances of a few wavelengths from the aperture, only the dipole far field terms are important. The power transferred by the small aperture (i.e., ratio of the time averaged power due to the equivalent dipole in the radiation zone to the incident power density) is

$$a_t = \left|\frac{\vec{E}\times\vec{H}^*}{\vec{E}_{inc}\times\vec{H}^*_{inc}}\right|^2 = \frac{k^4 d^6}{36\pi^2 X^2}\ .$$

In decibels and units of wavelength λ, this expression reduces to

$$A_t = 60\log_{10}\frac{d}{\lambda} - 20\log_{10}\frac{X}{\lambda} + 6.42\,.$$

For this expression, small aperture theory requires $d/\lambda \ll 1$, and in the radiation zone, $X/\lambda \gg 1$. Polarizabilities for a variety of other shapes have been calculated [13]. In most cases, the polarizabilities are not significantly different from that of a circular aperture of equal area.

The previous result shows that for small aperture Fraunhaufer diffraction, the transmitted power loss is substantial when the aperture is electrically small. This is not the case when, for example, a small aperture is backed by conducting materials that in effect form a resonant cavity [14, 15, 16, 17]. Analytical transmission line models have been used to calculate the *shielding effectiveness* SE of a rectangular metallic enclosure with a rectangular aperture. *SE* is defined as

$$SE = -20\log_{10}\left|\frac{\vec{E}(\vec{X})}{\vec{E}_0(\vec{X})}\right|$$

where $\vec{E}$ is the electric field at the observation point $\vec{X}$ inside of the enclosure and $\vec{E}_0$ is the electric field at the observation point assuming free space propagation. Measurements presented in [16] show that for a slot aperture with dimensions 100×5 mm in a rectangular box of dimensions 300×120×300 mm, the measured *SE* drops to only a few dB above 0 at 650 MHz and the analytical model predicts worst case *SE* values of −40 dB at around 700 MHz. Hence, apertures in "small" enclosures, and/or circumstances where metallic objects are near the aperture will require special analysis to determine if resonant behavior will result in significant field enhancements (over the small aperture theory) at frequencies within the threat range.

2.3 A Method for Estimating the Exterior to Interior Power Loss

The results presented above show that electromagnetic radiation can readily penetrate typical building walls that are poor conductors (i.e., suffering at most only a few dB of attenuation) and/or electrically large apertures such as doors and windows at various frequencies in the microwave band. The frequencies that exhibit worst case (i.e., maximum) penetration will depend on the materials and construction methods. While the infinite slab model is an idealization of a building wall, it is expected that the existence of wall boundaries, edges, corners, etc. will probably not reduce worst case penetration levels over a broad range of frequencies. However, such features will likely alter the frequency dependence of the transmitted power. In general, for typical masonry, wood, reinforced concrete, and similar structures made of materials with conductivities of a few mS/m or less, there will likely be significant penetration at several microwave frequencies, and hence the possibility of strong electromagnetic coupling into most structures should be anticipated. In what follows, we develop a statistical model that can be used to estimate worst case power levels that may exist within a cluttered room that has been penetrated by a narrow band of microwave radiation.

Once electromagnetic radiation penetrates a room, the fields are scattered, reflected, and diffracted by a variety of objects (equipment, furnishings, walls, etc.) inside of the room. The interior field structure can be very complicated and performing a detailed analysis of the power levels throughout a room is at best a difficult task. Since we are concerned here with estimating the worst case threat potential, a more practical approach is to use a statistical characterization of the indoor propagation channel for narrowband RF signals. The subject of indoor propagation at microwave frequencies has been studied by researchers for many years (see e.g., [18, 19]).

The model described here is applicable to situations where the interior of the building is loaded with many scattering objects, thus creating a strong multipath environment. The premise of the model is that when large areas of a building wall are illuminated by an RF device, the resulting signal within a room can be treated as originating from elemental sources over the illuminated wall area. In strong multipath environments, the signal from each source is subjected to random scattering. The phase of each signal is random and therefore each source can be considered as independent, in which case the total signal power is the sum of the signal power from each elemental source.

Following [20], the power level at a location inside of a room due to an elemental source within the room is modeled as the superposition of two processes: a multipath (small scale or *fast*) fading process superimposed upon a power (large scale or *slow*) fading process which can vary depending on a host of factors such as building construction and geometry, room characteristics and use, RF device type, deployment, etc. In situations where there are many multipath components that are about the same size, as would be expected in a room loaded with a variety of scatterers, the fast fading component is modeled as a multiplicative process that follows a *Rayleigh Law.* There are numerous studies that provide an empirical justification for modeling indoor fast fading as Rayleigh (see e.g., [21-24]). In cases where there is a strong direct signal, the fast fading component would consist of a direct plus a Rayleigh distributed signal which is characterized by Nakagami-Rice statistics.

In decibels relative to a unit of power (e.g., dBm), the power (or amplitude) at some point within the room can be written as

$$W = W_0 + R$$

where W_0 is a *smoothed* version of W and the residual R represents small scale variations due to interactions with the room and its contents. The variable $R = R(t,x,f)$ is in general a random function of time t, position x, and frequency f, and has a median value of 0 dB. The addition of quantiles in decibels implies a multiplicative relationship between the corresponding amplitudes indicating that the random function R acts as a frequency transfer function as would be expected for a severe multipath environment. As described in [20], the first-order statistics of R are given by

$$Pr\{R > \rho\} = 2^{-10^{\rho/10}}$$

which is referred to as the *Rayleigh decibel distribution*. This distribution has no parameters, a mean of 0.92 dB, a standard deviation of 5.57 dB, and an interdecile range of 13.40 dB. Note that with this model, the more general case of multipath plus a strong direct signal can readily be approximated using a *Weibull distribution* for $\boldsymbol{R}$ as described in [20].

Following [20] the quantity $\boldsymbol{W_0}$ can also be treated as a random variable depending on a parameter loosely described as situation. Here, the term situation is used to cover circumstances for which the contributions to the variability are significant, but difficult or impossible to quantify. It is envisioned that situation could apply to room-to-room variations, building type, construction, and use, and a variety of source parameters such as RF device type and deployment.

Published statistics based on indoor propagation measurements in factories and offices [21, 25] at UHF frequencies show that depending on the situation, Rayleigh or Nakagami-Rice statistics provide a reasonable approximation to indoor propagation measurements. In [21], it was found that the cumulative distribution of many small scale fading measurements in factory environments justify the assumption of a Rayleigh law. In both environments, small scale fading was best approximated by Nakagami-Rice statistics when the line-of-sight path was not obstructed and there was only light to moderate clutter. Nakagami-Rice distributions are typically characterized by the ratio of the direct to scattered signal power, usually denoted in decibels as $\boldsymbol{K}$. $\boldsymbol{K}$ values of 6-10 dB have been measured in a variety of indoor environments reported as having line-of-sight propagation paths with light to moderate clutter [21, 25, 26].

More recently, a numerical analysis software tool was used to calculate indoor propagation statistics for a Hertzian dipole source emitting a 2.4 GHz signal into a room loaded with many scattering objects and surfaces [27]. The primary purpose of this effort was to evaluate the efficacy of using the tool in predicting field strength variations for indoor environments. In particular, the software tool was used to simulate electromagnetic fields in a laboratory described as a harsh multipath environment with concrete exterior walls, glass windows, various partitions consisting of sheetrock over metal studs, concrete reinforced columns, and furnishings and equipment consistent with the function of the laboratory. The results of this study are useful for our purposes since they give detailed statistical data and show that severe multipath can result in significant field enhancements (relative to free space propagation) within a room.

The results of [27] are given in terms of a random variable called *room gain* which is defined as the ratio of the calculated electric field amplitude (using the software tool) to the electric field amplitude that would be present at the same location assuming free space propagation. In terms of our model, the median room gain can be associated with $\boldsymbol{W_0}$ (relative to the power based on a free space propagation law) and the variations relative to the median would correspond to $\boldsymbol{R}$. Room gain statistics are given for several transmitter locations, both near walls and in the center of the room. Depending on the transmitter location, the mean value of room gain is reported to be 4-8 dB above free space with standard deviations of 4.9-5.2 dB. It is interesting to note that while the mean value changes by several dB depending on antenna location, the standard deviation changes only slightly as would be expected with the Rayleigh small scale fading model described earlier. Furthermore, the reported standard deviation is reasonably close to the expected 5.57 dB for Rayleigh fading. While the data in [27] were fitted with lognormal distributions, it appears that the Rayleigh decibel distribution would also provide a reasonable fit. Also, statistics resulting from measurements of several different indoor paths [26] show that obstructed paths typically have standard deviations of 5.0-5.6 dB and mean values of 1-2 dB as would be expected for a Rayleigh distribution. Given these data and the physical basis for Rayleigh fading in a severe multipath environment, the assumption of Rayleigh fast fading appears to be justified.

2.3.1 Estimation of Exterior to Interior Power Loss

For equipment located near the illuminated wall or along a line-of-sight path with light to moderate clutter, the narrowband signal power can be characterized by Nakagami-Rice statistics with K values of about 6-10 dB. In such cases, the mean signal power at a point within the room will be roughly equal to power transmitted less free-space propagation losses (from the RF device to a point inside of the building) and any exterior wall attenuation. For equipment located farther into the room where the direct signal is very weak and multipath dominates, we will use the concepts described above to estimate worst case signal amplitudes.

To this end, the illuminated portion of the wall is divided into elemental isotropic radiators each occupying an area dA with power equal to $s_e dA/a_w$, where s_e is the power density at the exterior of the building wall and a_w is the wall attenuation. The power density at a location $\vec{x}$ within the room due to a point source at $\vec{x}_s$ is

$$ds(\vec{x}_r) = g_{rm} \frac{s_e\, dA}{4\pi\, a_w\, |\vec{x}_s - \vec{x}|^2}$$

where g_{rm} is the room gain (described above). We now assume that because of multipath, the signals received from each elemental source are essentially uncorrelated and hence the power density at $\vec{x}$ due to all sources is obtained by summing over the illuminated area A_0

$$s(\vec{x}_r) = g_{rm} \frac{s_e}{4\pi\, a_w} \int_{A_0} \frac{dA}{|\vec{x}_s - \vec{x}|^2}.$$

Since we are interested in worst case estimates we assume that the illuminated area is circular with radius r_0 and we need only calculate the threat along a line from the RF device through the center of the illuminated area. With these simplifying assumptions, the integral can readily be evaluated for interior locations along this line. Using cylindrical coordinates, where the z-axis is normal to the center of the illuminated circular area and z denotes the distance to an observation point within the room we have

$$h = \frac{1}{4\pi}\int_{A_0} \frac{dA}{|\vec{x} - \vec{x}_s|^2} = \frac{1}{4\pi}\int_0^{2\pi}\int_0^{r_0} \frac{r\,dr\,d\phi}{r^2 + z^2} = \frac{1}{4}\log_e\left(\frac{r_0^2}{z^2} + 1\right).$$

Using upper case letters to denote quantities in decibels, the interior power density is written as

$$S = G_{rm} + S_e - A_w + H.$$

Figure 8 shows H as a function of r_0^2/z^2. The quantity S has small scale variations that follow a Rayleigh law and large scale variations that depend on what was previously described as situation.

The mean power loss from the exterior illuminated area to the interior of the room is

$$\bar{A} = S_e - \bar{S} = A_w - \bar{G}_{rm} - H$$

where the bar above the symbol denotes average.

As an example, consider the case where the RF beam covers the entire exterior wall (i.e., r_0 is equal to half of the height of the exterior room wall). If the severe multipath assumption applies for $z \geq r_0/2$ we have $H = -4$ dB at $z = r_0/2$, and then decreasing with distance into the room as shown in Figure 8. For the situation described in [27], $\bar{G}_{rm} \approx 6$ dB, and hence, the worst case (i.e., smallest) mean power loss for obstructed portions of the room is

$$\bar{A} = A_w - 2.$$

Hence if the wall loss is nominally 2 dB or less at some frequencies over the bandwidth of the RF device, little if any shielding can be expected even in areas where the direct path is obstructed, and in fact, power enhancements are probable.

3. VULNERABILITY OF CELLULAR BASE STATIONS

An overview of cellular base stations is given in [1]. Briefly, a base station consists of an antenna (or array of antennas), an elevated mount (tower, rooftop, hilltop), an equipment enclosure (box, shed, building), a cable connection between the antenna and equipment enclosure, and either a cable, fiber, or microwave link to a mobile telephone switching office. As explained in [1], expected entry

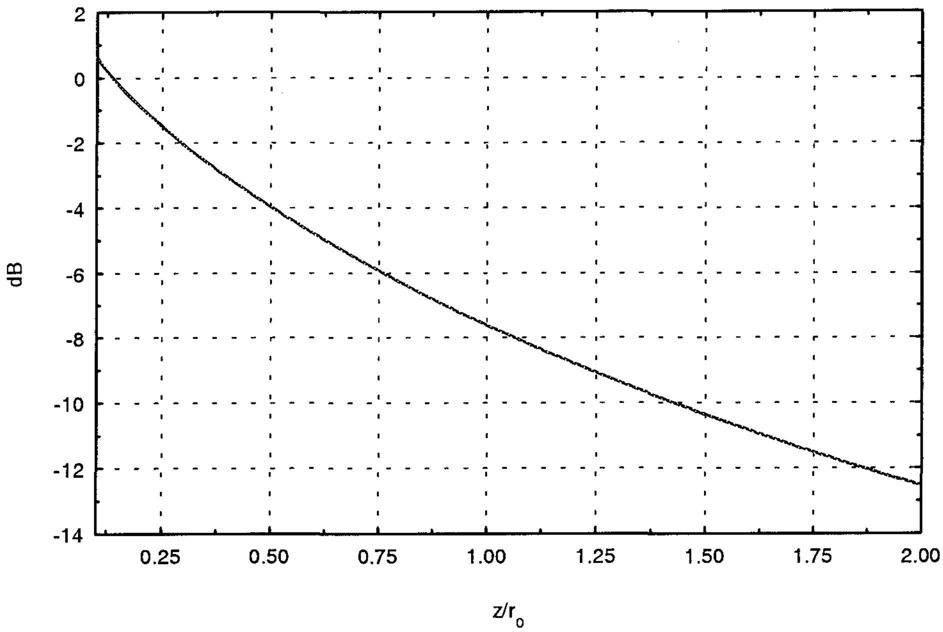

Figure 8. ***H*** as a function of distance from the illuminated wall relative to the radius of the illuminated portion of the wall.

points for RF radiation are the antenna, the connecting cable, and the equipment enclosure. Because antennas are intentional receivers of RF energy, the direct antenna coupling (or front door coupling) is expected to dominate the cable coupling and equipment enclosure coupling (back door couplings). These latter couplings depend on the shielding properties of the cable and enclosure, whereas the front door coupling depends on the antenna pattern.

Base stations are equipped with some form of lightning protection in the form of low-impedance ground paths that shunt transient currents away from the antennas, cables, and RF equipment. Protective measures generally take the form of grounding of exposed components and the use of surge protectors in cables. Although the base station grounding system may provide some protection against currents induced by high intensity RF fields, it is expected that in worst case scenarios, the signals generated by RF devices will follow the same path as the desired signals, and the grounding system will offer little protection. Thus, the primary threat to the base station is RF energy that is collected by the antenna and flows into the RF equipment.

Cellular base station antenna patterns are typically sectoral in the horizontal plane, with 3-dB beamwidths of 80 to 90 degrees in azimuth. In elevation the 3-dB beamwidths are typically 7½ to 15 degrees. A nominal antenna gain is 16 dBi. Antennas consist of metallic elements that are not expected to be affected by high intensity RF fields. Proper impedance matching between the antenna and its load (typically 50 ohm RF equipment) is necessary to achieve maximum power transfer. Since most matching circuits are passive devices, they are also expected to be unaffected by high intensity RF fields. Cellular base station antennas are therefore not expected to be damaged by high incident field levels.

As explained above, the main RF threat to base stations is direct coupling via the antennas. Since the antennas themselves are not expected to be vulnerable, it is the RF power that can damage (or degrade the performance of) the RF equipment that will be the determining factor for base station vulnerability. The signals received by a base station from mobile units are often very weak, and low noise amplifiers (LNAs) are therefore placed between the antennas and the receiver circuits. These amplifiers can be damaged (or suffer a loss of linearity and therefore experience degraded performance) if overloaded.

Loss of linearity is normally specified in terms of the 1-dB compression point (the point at which the amplifier gain as a function of input power deviates from linearity by 1 dB), referenced to the power at the amplifier output. A typical LNA has a 1-dB compression point of approximately 20 dBm and a gain of approximately 30 dB, so that the amplifier performance is degraded at an input power of approximately -10 dBm. One expects physical damage (burnout) at power levels of 20 to 40 dB greater than the 1-dB compression point, or an input power of approximately 10 to 30 dBm. These numbers are based on discussions with service providers, and may vary somewhat with different equipment from various manufacturers. However, it is worth noting that a study of the high power microwave vulnerability of electronic components commonly used in weapons systems yielded comparable numbers [28].

Overloading of the LNAs is avoided under normal conditions by limiting the power output of the mobile users and by placing narrowband RF filters between the antennas and the amplifiers. These front-end filters limit the out-of-band power received by the antenna from unintended sources. The filters accomplish this by acting as resonant cavities that can be tuned to the desired frequency band. Such filters function as duplexers; that is, they filter both transmitted and received signals. Since the transmitted power levels are much higher than the received power, the overload thresholds for these filters are specified in terms of transmit power, and are typically on the order of 1 kW. Thus, it is expected that the front-end filters will remain intact at power levels that will damage the LNAs.

The numbers cited above are all based on in-band power levels. The bandwidths for cellular and PCS services vary from approximately 5 MHz to 45 MHz, which are relatively narrowband for carrier frequencies in the 900- and 1800-MHz bands. On the other hand, some RF devices transmit ultrawideband signals [3,4], which may cause one to question the relevance of narrowband numbers for vulnerability assessments. However, because the front-end filters are expected to remain intact at power levels that will damage the front-end electronics, this damage will occur as a result of in-band power. It is therefore appropriate to use these in-band specifications to assess vulnerability to high power fields, including those generated by ultrawideband devices.

4. ANALYSIS TOOLS

In Sections 2 and 3, models of the transfer of RF energy into structures and cellular base stations were described. These models will now be used to develop tools that can be used to assess the vulnerability of telecommunications equipment to RF devices.

4.1 Buildings and Enclosures

In the case of telecommunications equipment housed inside a building or other enclosure, RF energy is not intentionally being collected (there is no receive antenna). One therefore cannot define a received power, which requires an effective antenna aperture and antenna gain. The penetration of RF energy into a structure will therefore be described in terms of power density (power per unit area) at a point inside the structure.

As described in Section 2, when RF energy propagates inside a structure, multipath propagation is expected to occur due to diffraction, reflections, and scattering (due to walls and objects inside of the structure). Thus, the RF power at a point inside the structure will in general consist of a combination of power from the direct path (from the source to the equipment) and power from multipath. One can therefore distinguish two different cases, depending on whether there is a direct path or whether the direct path is obstructed.

In the first case there is a direct path, which could occur, for example, when equipment is located near an exterior wall that is illuminated by RF energy. In this case, one expects that the power density at points inside the structure is a random function of position that obeys Rice-Nakagami statistics. The probability density function for the amplitude of such a process can be written as [29]

$$p(a) = \frac{a}{w_m} e^{-K - \frac{a^2}{2w_m}} I_0(2aK),$$

where a is the amplitude, w_m is the power in the multipath component, K is the so-called Ricean K-factor, defined as the ratio of the power in the direct component to the power in the multipath component, and I_0 is the modified Bessel function of the first kind of order zero.

The mean power of this process is the sum of the powers in the direct and multipath components. Thus, relative to the power density of the direct component, the total mean power density of the random process is $1 + 1/K$. This can be viewed as a room gain g_{rm}, because it is the ratio of the actual power density at a point to the power density that would be observed if the structure were absent. Using upper case letters to denote quantities in decibels, one can therefore express the power density at points inside the structure as

$$S = S_e - A_w + G_{rm},$$

where the quantities S, S_e, and A_w have the same meanings as in Section 2, and

$$G_{rm} = 10\log_{10}(1 + 1/K)\,.$$

The power density s_e at the exterior of the building wall is the power of the source (RF device) divided by the cross-sectional area of the RF beam. Equivalently, if the power transmitted by the device is p, then

$$s_e = \frac{p g_t}{4\pi\,\xi^2}$$

where ξ is the distance from the device to the exterior wall of the building and g_t is the directive gain of the device.

From this point of view, the second case, in which the direct path is obstructed, corresponds to a singular limit. In this limit, the power in the direct component tends to zero, the K-factor vanishes, and the room gain tends to infinity. The power observed at a point inside the structure can therefore be viewed as the product of a vanishing direct power and an infinite room gain. The value of this limit can be defined by the analysis at the end of Section 2, that is,

$$S = S_e - A_w + G_{rm} + H\,,$$

where G_{rm} is now the room gain that follows from the Rayleigh decibel distribution, as discussed above.

These expressions can be used to estimate the power density inside of a structure, in terms of the power of the RF device and its distance from the structure. However, as pointed out above, for typical building materials and RF frequencies, there may be essentially no shielding, whether or not the direct path is obstructed.

4.2 Cellular Base Stations

The vulnerability of cellular base stations can be analyzed in terms of the power delivered to the LNA via front door coupling through the receive antenna. This received power, denoted by p_r, can be determined using

$$p_r = \frac{p_t g_r g_t \lambda}{(4\pi\,\zeta)^2}$$

where p_t is the power transmitted by the RF device, g_t and g_r are the transmit and receive antenna gains, ζ is the antenna separation, and λ is the free space wavelength. In terms of decibels, this may be written as

$$P_r(dBm) = P_t(dBm) + G_t(dBi) + G_r(dBi) - 20\log_{10}(f(MHz)) - 20\log_{10}(\zeta(m)) + 28 \,.$$

This expression indicates that base stations are quite vulnerable to RF devices. For example, using a nominal gain of 16 dBi for the receive antenna, this expression implies that even a 1 kW device with no directive gain at a distance of 100 m and a frequency of 1 GHz would seriously overload an LNA with a 1-dB compression point of -10 dBm at the input.

5. SUMMARY

The analyses presented above indicate that structures made out of typical building materials offer little, if any, protection from high intensity RF fields. In some instances the presence of the structure may actually increase field strengths due to multipath effects. Cellular base stations are vulnerable to RF devices via front door coupling through the receive antenna.

Expressions have been derived that enable one to estimate the worst case power densities inside structures and the received power levels in cellular base stations. More quantitative predictions of field strengths can be made, but require detailed analyses on a case-by-case basis, taking into account frequency, the precise location of equipment inside a building, details of the structure, etc. The tools required for such analyses, including both analytical and numerical techniques, are currently available. These techniques have been briefly discussed in the report and are cited in the references.

6. REFERENCES

[1] P. Wilson, E. Haakinson and R. Dalke, "Vulnerability of wireline and cellular telecommunications networks to high power radio frequency fields," NTIA Report 01-382, Nov. 2000.

[2] M. Wik, R. Gardner and W. Radasky, "Electromagnetic terrorism and adverse effects of high power electromagnetic environments," in *Proc. 13th Intl. Zurich Symp. and Techn. Exhb. on EMC*," Zurich, Switzerland, 1999, pp. 181-185.

[3] R. Schweitzer and T. McCune, "Radio frequency weapons: The emerging threat and policy implications," report provided to Joint Program Office for Special Technology Countermeasures by Eagan, McAllister Associates, Inc. under Contract No. N39986-97-M-7184, Oct. 1998.

[4] J. Linder, W. Graham, M. Hewitt and T. Skucas, "Radio frequency, electromagnetic pulse, and high-power microwave weapons - threats, risks, and technology: An open-source assessment," report provided to Joint Program Office for Special Technology Countermeasures by National Security Research under Contract No. N39986-97-M-7241, Aug. 1997.

[5] J. A. Stratton, *Electromagnetic Theory*, New York: McGraw Hill Book Company, 1941, pp. 511-513.

[6] R. A. Dalke, et al., "Effects of reinforced concrete structures on RF communications," *IEEE Trans. on EMC,* vol. 42, no. 4, pp. 486-496, Nov. 2000.

[7] C. L. Holloway, M. G. Cotton, and P. McKenna, "A model for predicting the power delay profile characteristics inside a room," *IEEE Trans. on Veh. Technol.*, vol. 48, no. 4, pp. 1110-1120, Jul. 1999.

[8] J. B. Andersen, T. S. Rappaport, and S. Yoshida, "Propagation measurements and models for wireless communication channels," *IEEE Communications Magazine*, pp. 42-49, Jan. 1995.

[9] M. Born and E. Wolf, *Physical Optics,* New York: Pergamon Press, 1959, ch. 8.

[10] K. D. Mielenz, "Algorithms for Fresnel diffraction at rectangular and circular apertures," *Journal of Research of the National Institute of Standards and Technology*, vol. 103, no. 5, pp. 497-509, Sep.-Oct. 1998.

[11] D. E. Dauger, "Simulation and study of Fresnel diffraction for arbitrary two-dimensional apertures," *Computers in Physics*, vol. 10, no. 6, pp 591-604, Nov./Dec. 1996.

[12] H. A. Bethe, "Theory of diffraction by small holes," *Phys. Rev.,* vol. 66, pp. 163-182, Oct. 1944.

[13] K. S. H. Lee, Ed., *EMP Interaction: Principles, Techniques, and Reference Data,* New York: Hemisphere Publishing Corporation, 1968, pp. 436-454.

[14] M. P. Robinson, et al., "Analytical formulation for the shielding effectiveness of enclosures with apertures," *IEEE Trans. on Electmagn. Compat.* vol. 40, no. 3, pp. 240-248, Aug. 1998.

[15] H. H. Park, et al., "FDTD analysis of electromagnetic penetration into a rectangular enclosure with multiple rectangular apertures,"*Microwave and Optical Technology Letters,* vol. 22, no. 3, pp. 288-191, Aug. 1999.

[16] R. Azaro, et al., "Evaluation of the effects of an external incident electromagnetic wave on metallic enclosures with rectangular apertures," *Microwave and Optical Technology Letters,* vol. 28, no. 5, pp. 288-191, Mar. 2001.

[17] K. Y. Kabalan, et al., "Electromagnetic coupling to conducting objects behind apertures in a conducting body," *Radio Science,* vol. 32, no. 3, pp. 881-898, May-Jun. 1997.

[18] O. Hashemi, "The indoor radio propagation channel," *Proc. of the IEEE*, vol. 81, no. 7, pp. 943-968, Jul. 1993.

[19] A. F. Toledo and A. M. D. Turkmani, "Propagation into and within buildings at 900, 1800, and 2300 MHz," in *Proc. of the IEEE vehicular technology society 42nd VTS conference, vol. 2*, Denver, CO., May 10-13, pp. 633-636.

[20] G. Hufford, "A general model for signal level variability," *IEEE Journal on Selected Areas in Communications*, vol. SAC-5, no. 2, pp. 299-301, Feb. 1987.

[21] T. S. Rappaport and C. D. McGillem, "UHF fading in factories," *IEEE Journal on Selected Areas in Communications*, vol. 7, no. 1, pp. 40-48, Jan. 1989.

[22] P. Yegani and C. D. McGillem, "A statistical model for line-of-sight (LOS) factory radio channels," in *Proc. Vehicular Techn. Conf. VTC'89*, San Francisco, May 1989, pp. 496-503.

[23] H. H. Hoffman and D.C. Cox, "Attenuation of 900 MHz radio waves propagating into a metal building," *IEEE Trans. Antennas Propagt.*, vol. AP-30, no. 4, pp. 808-811, Jul. 1982.

[24] S. T. S. Chia and A. Baran, "900 MHz attenuation and bit error ratio measurements inside a modern office building," in *Proc. IEE Fifth Int. Conf. Mobile Radio Personal Commun.*, Warick, U.K., Dec. 1989 pp. 33-37.

[25] R. J. Bultitude, S. A. Mahmoud, and W. A. Sullivan, "A comparison of indoor radio propagation characteristics at 910 MHz and 1.75 GHz," *IEEE Journal on Selected Areas in Communications*, vol. 7, no. 1, pp. 20-30, Jan. 1989.

[26] R. Valenzuela, O. Landron, and D. L. Jacobs, "Estimating local mean signal strength of indoor multipath propagation,"*IEEE Trans. on Veh. Technol.*, vol. 46, no. 1, pp. 203-212, Feb. 1997.

[27] I. Bolanis, "Prediction of wireless communications systems performance in indoor applications," Master's Thesis, Naval Postgraduate School, Monterey, California, Dec. 2000.

[28] R. Antinone and W. Ng, "HPM testing of electronic components," Technical Report UCID-21687, Lawrence Livermore National Laboratory and BDM Corporation, May 1989.

[29] R. Janaswamy, *Radiowave Propagation and Smart Antennas for Wireless Communications,* Boston, MA: Kluwer Academic Publishers, 2001, ch. 4.

FORM **NTIA-29**
(4-80)

U.S. DEPARTMENT OF COMMERCE
NAT'L. TELECOMMUNICATIONS AND INFORMATION ADMINISTRATION

BIBLIOGRAPHIC DATA SHEET

	1. PUBLICATION NO.	2. Gov't Accession No.	3. Recipient's Accession No.
	NTIA 02-391		

4. TITLE AND SUBTITLE

ANALYSIS OF THE RF THREAT TO TELECOMMUNICATIONS SWITCHING STATIONS AND CELLULAR BASE STATIONS

5. Publication Date

6. Performing Organization Code

NTIA/ITS.T

7. AUTHOR(S)

John J. Lemmon and Roger A. Dalke

8. PERFORMING ORGANIZATION NAME AND ADDRESS

NTIA/ITS
325 Broadway
Boulder, CO 80305-3328

9. Project/Task/Work Unit No.

10. Contract/Grant No.

11. Sponsoring Organization Name and Address

NTIA
Herbert C. Hoover Building
1401 Constitution AVe. NW
Washington, DC 20230

12. Type of Report and Period Covered

13.

14. SUPPLEMENTARY NOTES

15. ABSTRACT *(A 200-word or less factual summary of most significant information. If document includes a significant bibliography or literature survey, mention it here.)*

The objective of this report is to assess the bulnerability of telecommunications switching stations and cellular base stations to high power electromagnetic radiation generated by an RF device. Analyses, measurements, and simulations of indoor propagation and the penetration of electromagnetic fields into structures indicate that typical buildigns provide little, if any, protection for telecommunications switching stations from high power electromagnetic fields. The front end electronics of cellular base stations are also vulnerable to damage from high intensity RF fields via front door coupling through the receive antennas. Tools to provide estimates of power densities inside of structures and the received power levels in cellular base stations are developed in this report. More quantitative predictions of field strengths inside structures require detailed analyses on a case-by-case basis. The techniques to carry out such analyses are currently available and are briefly discussed.

16. Key Words *(Alphabetical order, separated by semicolons)*

critical infrastructure protection, high power RF fields, telecommunications switching stations, cellular base stations, shielding, vulnerability

17. AVAILABILITY STATEMENT	18. Security Class. *(This report)*	20. Number of pages
☐ UNLIMITED.	19. Security Class. *(This page)*	21. Price:
☐ FOR OFFICIAL DISTRIBUTION.		

*U.S. GPO 2002-0-773-018/40205